

# LEGIBILITY NOTICE

A major purpose of the Technical Information Center is to provide the broadest dissemination possible of information contained in DOE's Research and Development Reports to business, industry, the academic community, and federal, state and local governments.

Although a small portion of this report is not reproducible, it is being made available to expedite the availability of information on the research discussed herein.

LA-UR--88-2376

DE88 014335

TITLE: THE EFFECTS OF SPATIALLY-VARYING SOIL PROPERTIES ON SOIL EROSION

AUTHOR(S): E. P. Springer  
T. W. Cundy

SUBMITTED TO: ASAE International Symposium on Modeling Agricultural, Forest,  
and Rangeland Hydrology  
December 12-13, 1988  
Chicago, Illinois

DISCLAIMER

This report was prepared as an account of work sponsored by an agency of the United States Government. Neither the United States Government nor any agency thereof, nor any of their employees, makes any warranty, express or implied, or assumes any legal liability or responsibility for the accuracy, completeness, or usefulness of any information, apparatus, product, or process disclosed, or represents that its use would not infringe privately owned rights. Reference herein to any specific commercial product, process, or service by trade name, trademark, manufacturer, or otherwise does not necessarily constitute or imply its endorsement, recommendation, or favoring by the United States Government or any agency thereof. The views and opinions of authors expressed herein do not necessarily state or reflect those of the United States Government or any agency thereof.

By acceptance of this article the publisher recognizes that the U.S. Government retains a nonexclusive, royalty-free license to publish or reproduce, the published form of this contribution or to allow others to do so, for U.S. Government purposes

The Los Alamos National Laboratory requests that the publisher identify this article as work performed under the auspices of the U.S. Department of Energy

DISTRIBUTION OF THIS DOCUMENT IS UNLIMITED

Los Alamos Los Alamos National Laboratory  
Los Alamos, New Mexico 87545

THE EFFECTS OF SPATIALLY-VARYING SOIL PROPERTIES  
ON SOIL EROSION

E. P. Springer\*

T. W. Cundy\*

Soil erosion is a major concern for agronomist, agricultural engineers, and land managers. The removal of soil may decrease site productivity while soil deposition can aggrade stream channels and fill reservoirs. In addition to being a major pollutant, eroded soil may be another source of water quality degradation. These factors make erosion prediction an important aspect in evaluating land-use alternatives.

Mathematical modeling of soil erosion must include surface runoff the dominant transport mechanism. Rainfall excess when routed over the surface, produces a distribution of velocities and depths in response to surface roughness, surface form or microtopography, and available water. The spatial distribution of velocities and depths strongly affects sediment delivery as well as the re-distribution of soil on the hillslope.

The objective of this study is to investigate the effects of only rainfall excess generation on erosion. In particular, we will illustrate the effects of spatial variation in saturated hydraulic conductivity ( $K_s$ ) on the spatial and temporal distributions of erosion resulting from overland flow. We will then use this as a basis to demonstrate the potential for bias in parameters estimated from field data.

---

E. P. Springer, Staff Member, Environmental Science Group, MS J495, Los Alamos National Laboratory, Los Alamos, NM 87545 and T. W. Cundy, Assoc. Prof., College of Forest Resources, AR-10, University of Washington, Seattle, WA 98195.

## BACKGROUND

Since the study by Nielsen et al. (1973), there has been considerable effort expended to understand the nature of spatially-varying soil properties, and their effects. In a seminal study Smith and Hebbert (1979) used the infiltration model from Smith and Parlange (1978) and kinematic wave overland flow routing to study the effects of spatially-varied infiltration parameters on overland flow. For the conditions of their study, Smith and Hebbert found that the concept of a single effective parameter set governing system response was inappropriate, i.e., some knowledge of the spatial variability of the soil parameters must be included, and the rainfall intensity was also important. This result was confirmed in subsequent studies of Fræze (1980) and Dagan and Bresler (1983). Smith and Hebbert (1979) also reported differences in runoff hydrographs depending on the orientation of  $K_s$  value along their simulated hillslopes. These differences imply differential erosion along the slope even though the mean and variance of  $K_s$  are identical. It is the differences in flow velocities and depths that are form the basis for this study.

The sensitivity of surface runoff to parameters in various infiltration equations have revealed that the conductivity parameters and antecedent moisture are the most sensitive (Brakensiek and Onstad 1977). Springer and Cundy (1987) showed for runoff from hillslopes with spatially-variable

infiltration parameters that for the Green and Ampt (1911) approximation the average suction head ( $S_{av}$ ) and saturated water content ( $\theta_s$ ) could be set to mean values with essentially no effect on the resulting hydrographs.

## MATHEMATICAL MODEL

### Geometry

The hillslopes used in these simulations is a rectangle with uniform width. One dimensional sheetflow is assumed for all simulations.

### Rainfall

Spatially uniform rainfall was used in all of the simulations. The rainfall was temporally varied based on the recent work of Woolhiser and Goodrich (1988) who found bias resulting from constant intensity rainfall. For simplicity a triangular rainfall pattern was used to describe the temporal variation. The duration and constant intensity for an event are specified and by solving for the area, the peak intensity can be calculated. The capability of describing many different unimodal rainfall hyetographs by adjusting the location of the apex by adjusting only one parameter is an advantage of the triangular distribution.

### Infiltration Modeling

Rainfall excess was calculated using the Green and Ampt (1911) infiltration equation. The rate form of this equation is

$$f(t) = K_o \left[ 1 + \frac{S_{av} (\theta_s - \theta_i)}{F(t)} \right] \quad (1)$$

where  $f(t)$  is the infiltration rate (cm/hr);  $K_o$  is the Green-Ampt conductivity (cm/hr);  $S_{av}$  is the average suction head (cm);  $\theta_s$  is the saturated volumetric water content;  $\theta_i$  is the initial volumetric water content; and  $F(t)$  is the cumulative infiltration (cm).

Infiltration under a flux boundary condition is composed of an initial period where the infiltration rate is equal to the rainfall intensity, and following ponding, infiltration is limited by the soil intake capacity (Mein and Larson 1973). Eggert (1976) and Chu (1978) developed a technique to solve Eq. 1 for an arbitrary rainfall hyetograph. Both techniques require testing at the end of each time interval ( $\Delta t$ ) to see if  $R(i)$  is greater than  $f$  assuming all rainfall in  $\Delta t$  will infiltrate. When  $f(t)$  is greater than  $R(i)$ , ponding has occurred in that interval and an interpolation is used to determine ponding time.

After ponding infiltration becomes capacity limited rather than supply limited until the input rate again drops below the infiltration capacity. The cumulative infiltration following ponding is determined using the cumulative form of Eq. 1 which is

$$K_o \Delta t = F(t) - S_{av} (\theta_s - \theta_i) \ln \left[ 1 + \frac{F(t)}{(\theta_s - \theta_i) S_{av}} \right] \quad (2)$$

where all parameters have been defined, and the time correction method suggested by Mein and Larson (1973) to correct for time to ponding is used. The infiltration rate following ponding is calculated as an average over a  $\Delta t$  time period. In equation form this is

$$\bar{f}_i = \frac{F(t_i) - F(t_{i-1})}{t_i - t_{i-2}} \quad (3)$$

where  $\bar{f}_i$  is the average infiltration rate (cm/hr). This procedure is particularly amenable to numerical solution techniques for the overland flow equations described below because the time domain is discretized into intervals for numerical solution.

Rainfall excess is calculated as the difference between the rainfall rate and average infiltration rate for an interval

$$q_e(i) = R_i - \bar{f}_i \quad (4)$$

where  $q_e(i)$  is the rainfall excess (cm/hr).

### Overland Flow

Overland routing of the rainfall excess uses the one-dimensional kinematic wave equation (Henderson and Wooding 1964). The spatially and temporally varying input requires a numerical solution. The continuity equation for a one-dimensional, rectangular channel of infinite width is

$$\frac{\partial h}{\partial t} + \frac{\partial q}{\partial x} = q_e \quad (5)$$

where  $h$ , is  $h(x,t)$ , is the depth of water (cm);  $q$ , is  $q(x,t)$ , is the flow per unit width ( $\text{cm}^2/\text{hr}$ ),  $q_e$ , is  $q_e(x,t)$ , is the lateral inflow ( $\text{cm}/\text{hr}$ ); and  $x,t$  are the space and time coordinates, respectively. The kinematic approximation assumes for the momentum equation that the friction slope is equal to the bed slope,  $S_o$ . So  $q$  can be described by

$$q = \alpha h^B \quad (6)$$

where  $\alpha$  is the slope-friction factor and  $B$  is the channel shape factor.

In this study the Chezy law was used for Eq. 6 so the parameters are

$$\alpha = C_h (S_o)^{1/2} \quad (7)$$

where  $C_h$  is the Chezy C for a given surface; and  $S_o$  is the bed slope, and  $B$  was set to a constant value of 1.5.

The numerical solution uses the implicit finite difference scheme of Li et al. (1975). In this scheme, Eq. 6 is inverted for  $h$  rather than  $q$ . A Newton method is used to solve the resulting nonlinear difference equations.

### Erosion

The continuity equation for sediment from an eroding surface is (Bennett 1974)

$$\frac{\partial(hC)}{\partial t} + \frac{\partial(qC)}{\partial x} = w \quad (8)$$



where  $c$  is the concentration ( $\text{gm}/\text{cm}^3$ );  $h$  is the depth of flow (cm);  $q$  is the flow per unit width ( $\text{cm}^2/\text{hr}$ ); and  $w$  is the source/sink term for sediment ( $\text{g}\cdot\text{cm}/\text{hr}$ ). On uniform slopes the available material for transport will be determined by the rill and interrill detachment (Foster and Meyer 1972; Foster et al. 1977). To illustrate the effects of spatially variable  $K_s$ . The assumption that sufficient material was available for transport or the transport capacity of the flow is the limiting factor.

The DuBoys transport equation (Simons and Senturk 1977) was used to calculate sediment transport. The equation is

$$Q_s = \phi \tau_b (\tau_b - \tau_c) \quad (9)$$

where  $Q_s$  is volume discharge of sediment per unit width ( $\text{cm}^2/\text{s}$ );  $\phi$  is a transport parameter ( $\text{cm}^6/\text{dyne}^2\text{-s}$ );  $\tau_b$  is the shear stress ( $\text{pgh}S_0$ ) ( $\text{g}/\text{cm}\cdot\text{s}^2$ ); and  $\tau_c$  is the critical shear stress ( $\text{g}/\text{cm}\cdot\text{s}^2$ ). Both  $\phi$  and  $\tau_c$  are functions of particle diameter. Equation 9 assumes cohesionless particles of a uniform size in its formulation.

The assumption of unlimited sediment supply means that Eq. (8) would not have to be solved. Sediment transport at each node was calculated using updated flow conditions for that time step and Eq. (10).

Soil erosion or deposition over a  $\Delta x$  is determined by the difference between the  $Q_s$  value upslope from the solution node and the  $Q_s$  value calculated at the current node. Only the transport capacity at a node is satisfied, and erosion or deposition are assumed to occur uniformly over

the  $\Delta x$  interval between adjacent nodes.

### EXPERIMENTAL APPROACH

The mathematical model described in the previous section forms the foundation of the analysis. In this section, details for the simulations are described.

The geometry of the hillslope is conceptualized in Fig. 1. The hypothetical hillslope is 100-m long and 1 m wide with a uniform slope of .05 was used for all simulations.

The slope is divided into 100 - 1 m x 1 m elements. An element is expanded from the hillslope in Fig. 1. The elements represent an arbitrary length scale that describe the spatial variation in  $K_s$  along the hillslope. Within this 1-m<sup>2</sup> block  $K_s$  takes a constant value with different  $K_s$  values between blocks. The length of the element should not be confused with the  $\Delta x$  values required for overland flow simulation. As shown in Fig. 1 there can be several  $\Delta x$  values within an element.

*Figure 1.*

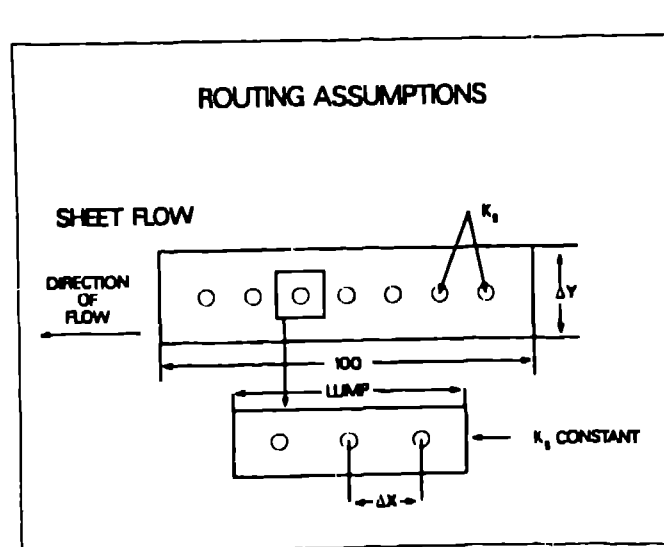


*Figure 1.*

The conductivity parameter has been found to be the most sensitive parameter when simulating rainfall-runoff (Brakensiek and Onstad 1977; Springer and Cundy 1987). This is the reason that  $K_s$  is the only spatially-varied input in the simulations. Results from field studies have indicated that the spatial distribution of  $K_s$  is log normal (Nielsen et al. 1973; Freeze 1975). An arithmetic mean of 2.54 cm/hr ( $\bar{K}_s$ ) was assumed for all simulations, and coefficients of variation (CV) were for the spatial distribution of  $K_s$  were 0.0, 0.2, and 0.8. This  $\bar{K}_s$  value is indicative of a sandy to sandy-loam texture class (Cosby et al. 1984) for the assumptions in the sediment transport model. Assuming a log normal distribution, two realizations of 100 values were generated (one for CV = 0.2 and one for CV = 0.8) using routines from the Statistical Analysis System package (SAS 1985). The random  $K_s$  values were located from the top to the bottom of the hillslope as they were generated.

Two parameters and the initial water content,  $\theta_1$ , are required to completely specify Eq. 1.  $S_{av}$  was set at 10.16 cm and the value from  $\theta_s$  is 0.40. Two values of  $\theta_1$  were arbitrarily chosen 0.2 and 0.3 to examine the effects of initial conditions.

Rainfall values were also selected as a function of  $\bar{K}_s$ . Total rainfall duration was 15 min., and two constant intensities,  $3 \bar{K}_s$  and  $6 \bar{K}_s$ , were used to characterize rainfall amounts. An isocetes triangle described the temporal rainfall pattern. The peak intensities occurred at 7.5 min with values of  $6 \bar{K}_s$  and  $12 K_s$  or twice the constant intensity value.

Overland flow requires a value for  $C_h$  in Eq. 7. The selected value of

3312.5 cm<sup>1/2</sup>s was taken from Rovey et al. (1977) for a surface with sparse vegetation. Again, this is in keeping with the sandy soil texture. The space and time increments were set for all simulations at 50 cm and 30s.

The transport parameter,  $\theta$ , and critical shear stress,  $\tau_c$ , were also given values representative of a sandy soil. A mean particle diameter of 0.5 mm was assumed and the values for  $\phi$  is .0011 cm<sup>6</sup>/dynes<sup>5</sup> and  $\tau_c$  is 10.46 gm/cm<sup>5</sup><sup>2</sup>.

All parameters are listed in Table 1.

A total of 12 simulations were conducted with two rainfall intensities, 2 antecedent moisture conditions, and three spatial patterns of  $K_s$ .

Table 1. Parameter values used in the simulations.

<u>Parameter</u>	<u>Value</u>	<u>Remarks</u>
Rainfall Duration	15 min	
Peak Rainfall Intensity	15.24 cm/hr	6 $\bar{K}_s$ ; total rain = 1.9 cm
Peak Rainfall Intensity	30.48 cm/hr	12 $\bar{K}_s$ ; total rain = 3.8 cm
$K_s$	$\bar{K}_s = 2.54$ cm/hr	mean value
CV ( $K_s$ )	.2 and .8	coefficient of variation
$S_{av}$ (cm)	10.16	Average suction head
$\theta_s$	0.40	Saturated water content
$\theta_i$	0.20, 0.30	Initial water contents
Chezy C (cm <sup>1/2</sup> /s)	3312.5	Roughness factor
B	1.5	Channel shape factor
$\phi$ (cm <sup>6</sup> /dynes-s)	.0011	Sediment transport factor
$\tau_c$ (gm/cm-s <sup>2</sup> )	10.46	Critical shear stress
$\Delta x$ (cm)	50.0	Space interval for solution
$\Delta t$ (s)	30.0	Time interval for solution

## RESULTS AND DISCUSSION

### Hillslope Simulations

Figure 2 is a three-dimensional plot of cumulative erosion versus distance at each time. A distance value of zero is the top of the slope. The response in Fig. 2 is for  $\theta_1 = 0.2$ ,  $CV = 0.2$ , and a peak intensity of 15.24 cm/hr or  $6 \bar{K}_s$ . Close inspection of Fig. 2 reveals an irregular response on the downslope direction. The differential erosion rates at each location are displayed in Fig. 3 using the same perspective as Fig. 2. Deposition is seen as those values below the zero line. As can be seen, deposition occurs at certain locations for essentially all time. Most of the erosion is occurring at the extreme upslope end because the flow is developing and sufficient transport capacity exist. At the middle and lower slope reaches, deposition and erosion become highly erratic in both space and time in response to the variable rainfall excess. By increasing the CV for  $K_s$ , created by high and low values of  $K_s$  an even more erratic response in the cumulative erosion can be observed in Fig. 4 with considerable deposition in the interval between 5000-7500 cm. This result is further illustrated in Fig. 5 which is a plot of the differential erosion rates for a  $CV = 0.8$ .

It is interesting to compare cumulative erosion from surfaces with variable  $K_s$  (Figs. 2 and 4) with the cumulative erosion from a surface that is described by a constant  $K_s$  ( $\bar{K}_s$ ) at all locations (Fig. 6).

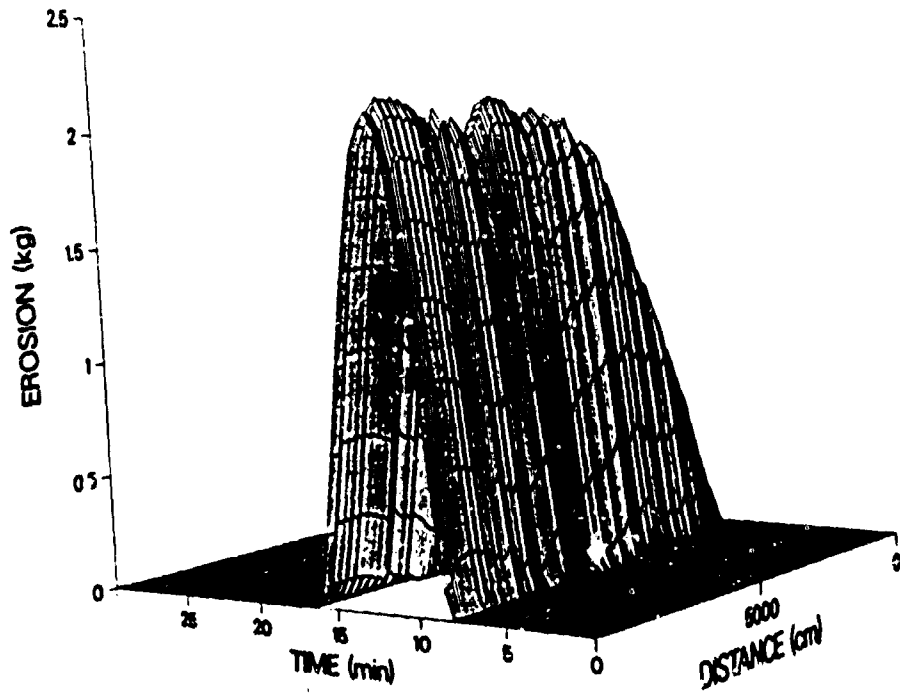


Figure 2.

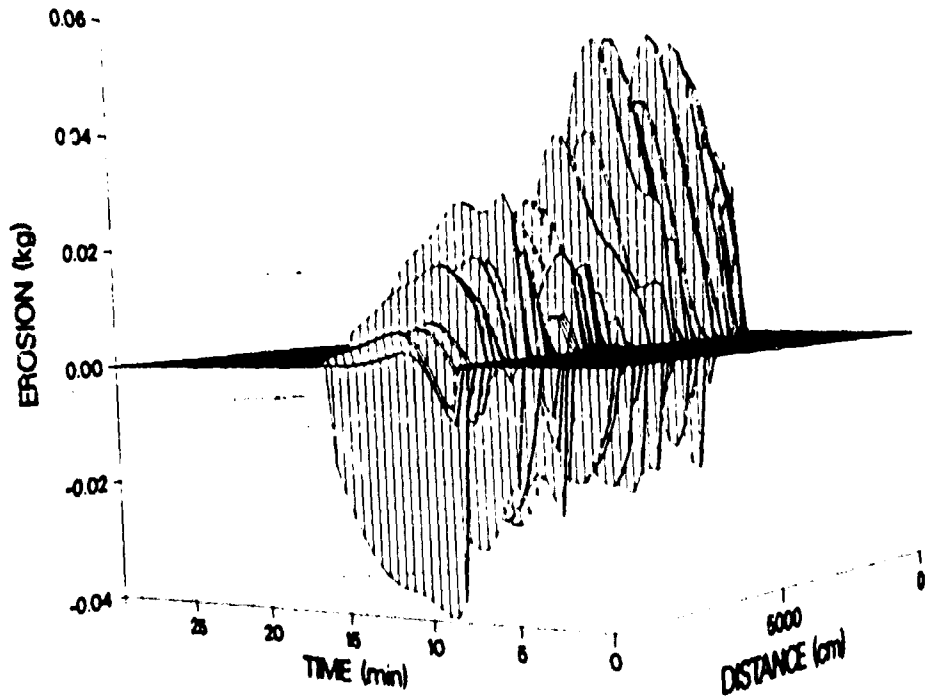


Figure 3.

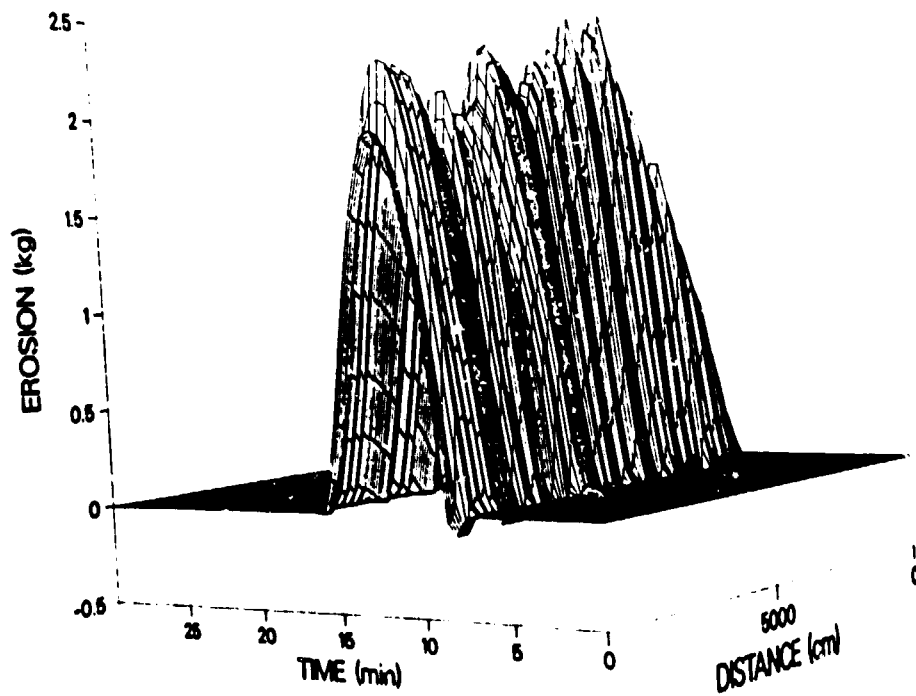


Figure 4.

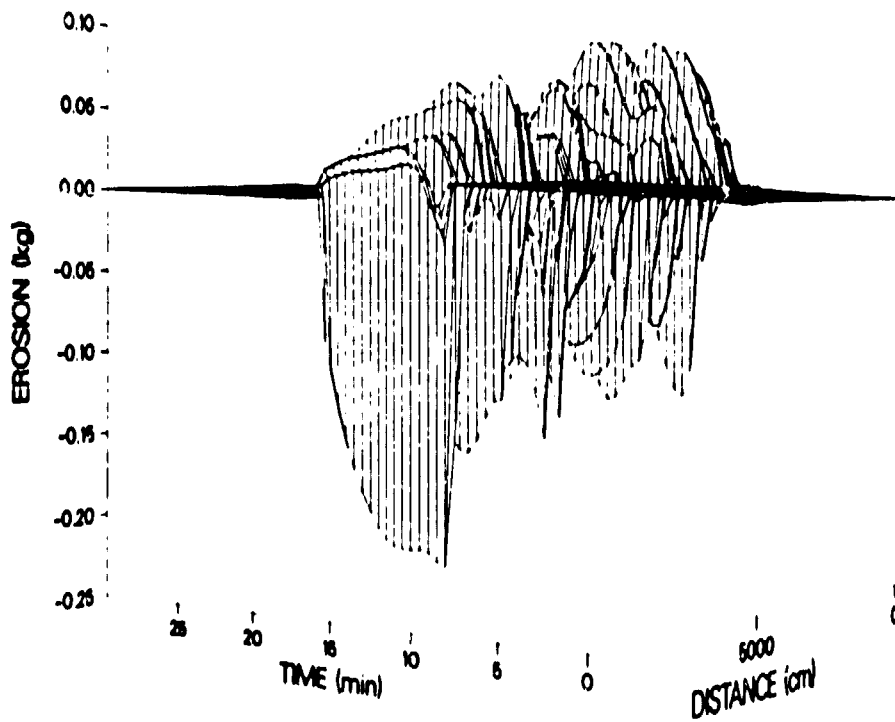


Figure 5.

Results in Fig. 6 are much smoother, and there is no erratic behavior. The plot of the differential erosion rates (Fig. 7) indicates little or no deposition along the slope. The obvious differences in the spatial and temporal responses of the constant versus spatially distributed surfaces for this system indicate the potential distortion that can occur when a single parameter set is used.

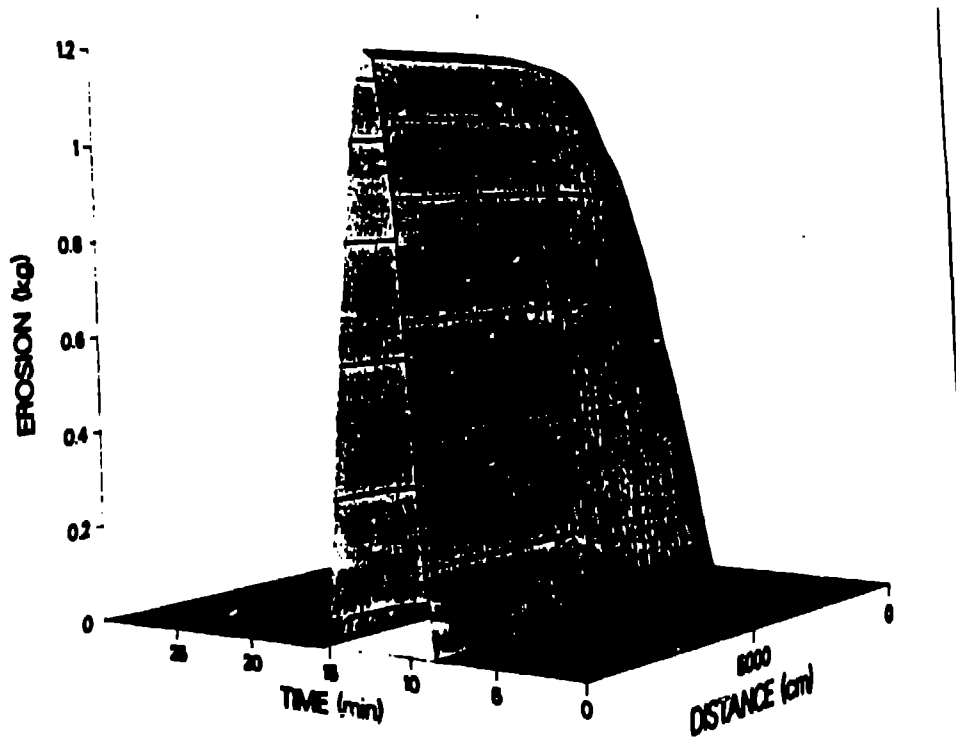


Figure 6.



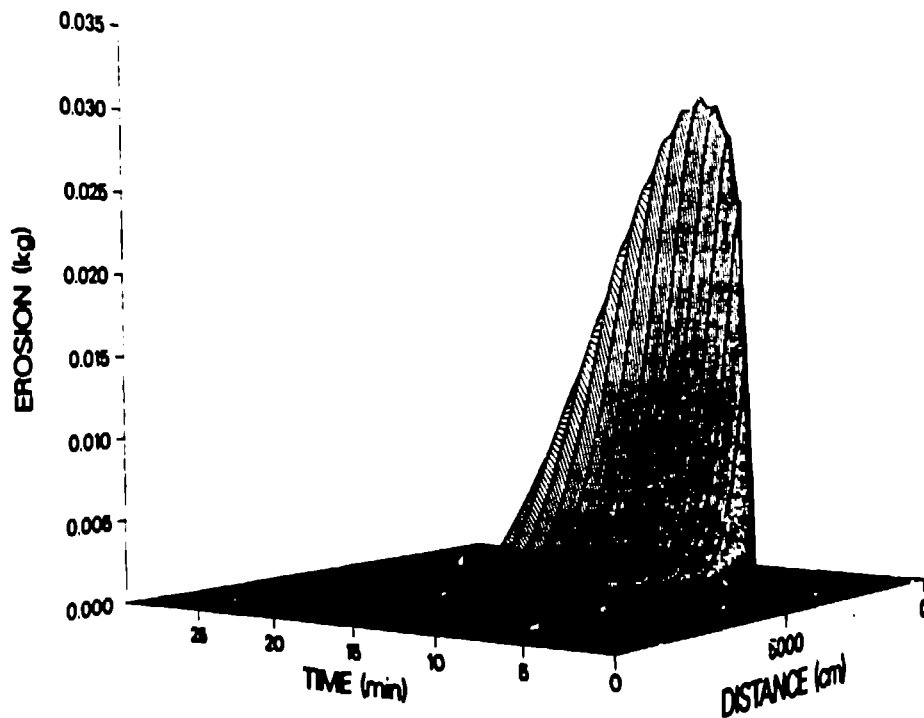


Figure 7.

These results are for a single rainfall intensity for two CVs of  $K_s$ . Another set of simulations was conducted at a rainfall intensity of twice the previous set. As in the previous simulations, responses for the mean or constant surface ( $CV = 0.0$ ) are consistent with a smoothly rising cumulative sediment graph for both initial moisture contents (Fig. 8). The introduction of a spatially variable  $K_s$  again revealed an irregular pattern of differential sediment transport in both space and time with the  $CV = 0.8$  (Fig. 9) exhibiting more variation along slope than the  $CV = 0.2$  (Fig. 10) simulations for a given antecedent water content.

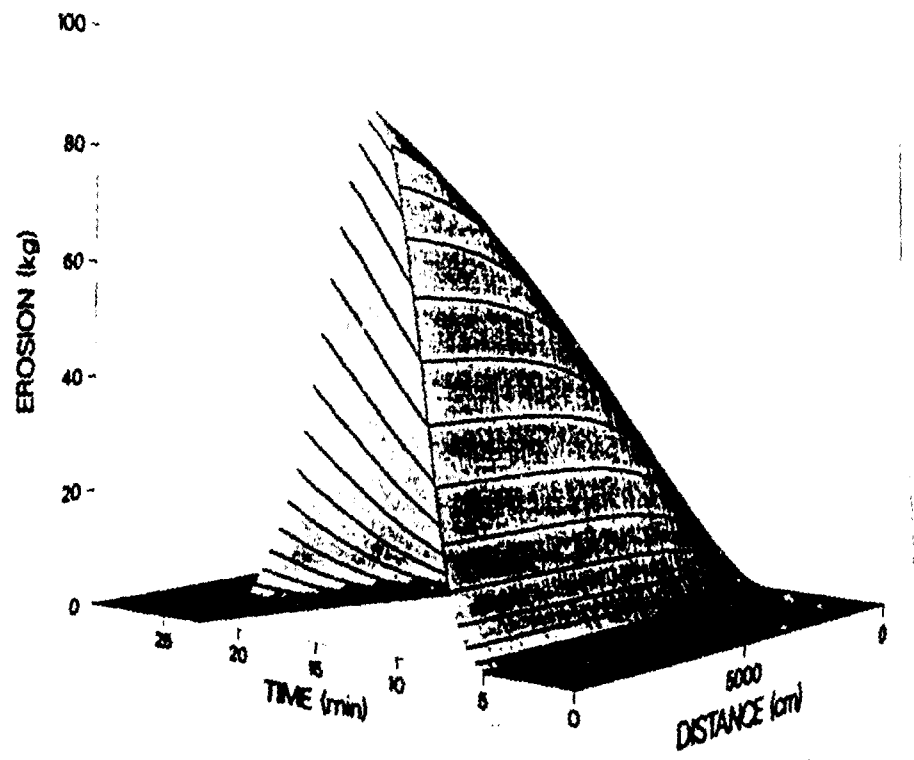


Figure 8.

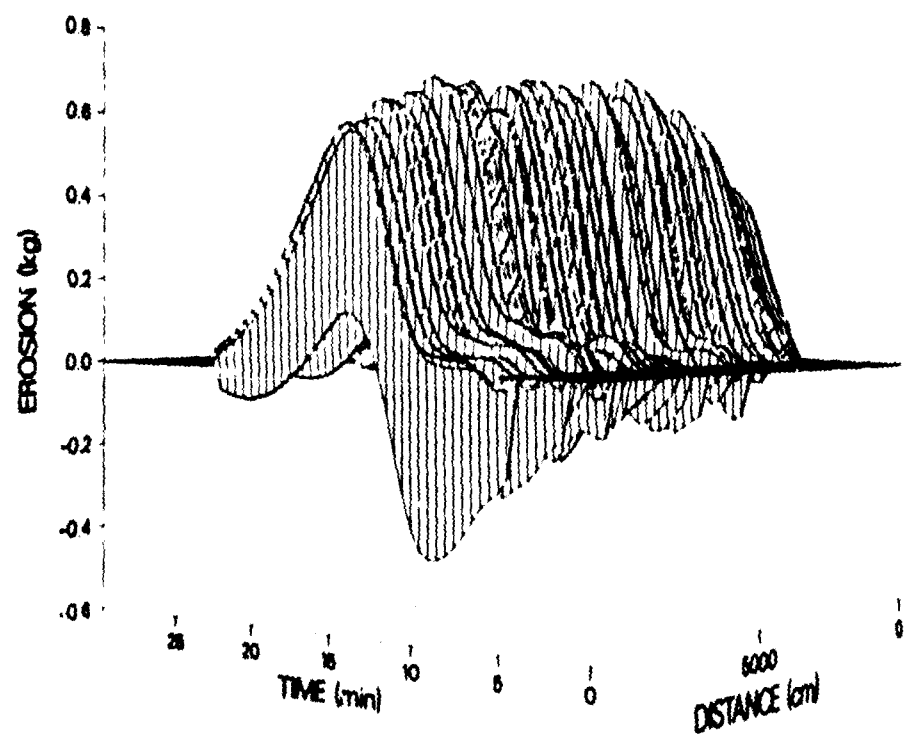


Figure 9.

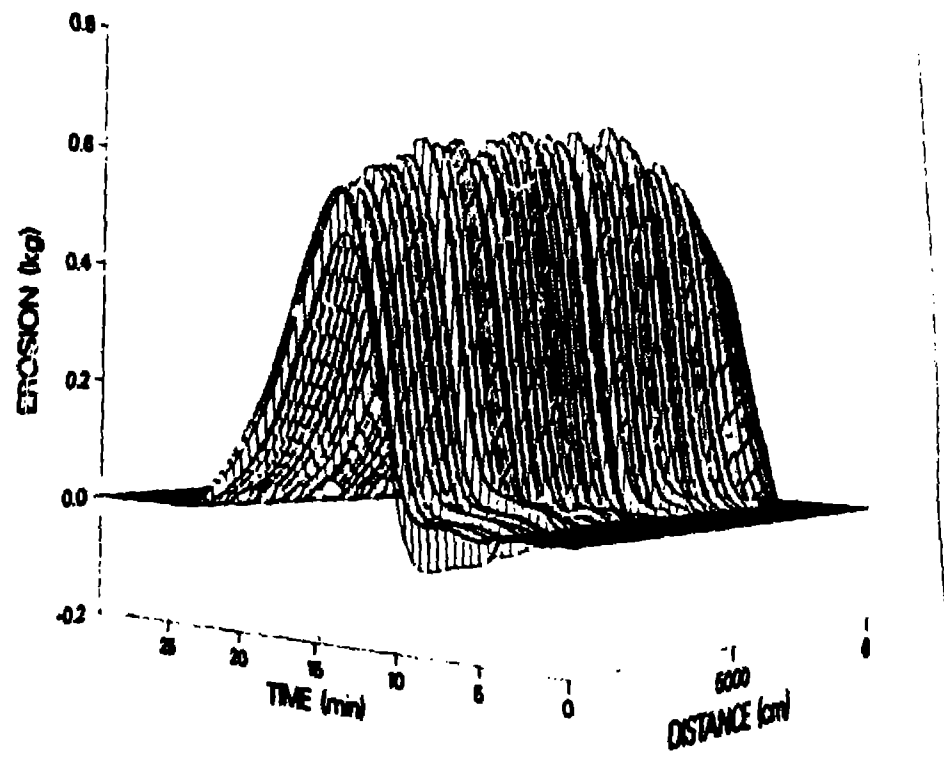


Figure 10.

When analyzing sediment transport from a plot with a rainfall simulator, the total soil loss is the variable most often collected and used. For the twelve simulations conducted the total sediment delivered is given in Table 2. Note that the simulations with variable  $K_n$  give higher total sediment yields than for the case with a constant mean  $K_n$ . This is consistent with previously reported results on runoff (Hawkins and Cundy 1987) and follows directly from the DuBoys model where sediment transport capacity is directly proportional to flow depth.

Table 2. Total sediment transport (kg) for the simulations.

P = 1.9 cm		
	$\theta_1 = 0.2$	$\theta_1 = 0.3$
CV = 0.0	9.5	72.0
CV = 0.2	19.2	97.4
CV = 0.8	17.0	91.1
P = 3.8 cm		
CV = 0.0	912.5	1228.1
CV = 0.2	997.5	1302.8
CV = 0.8	975.6	1274.2

### Implications for Parameter Estimation

These results have implications for estimating erosion parameters from field data. When conducting rainfall simulator experiments, the sediment graph or sediment concentration versus time is the response variable most often collected for parameter estimation purposes. In the analysis that follows, the sediment graphs for the simulations with  $P = 1.9$  cm,  $\theta_1 = 0.2$  and  $P = 3.8$  cm, and  $\theta_1 = 0.3$ , for  $CV = 0.2$  and  $CV = 0.8$  will be used to estimate the transport parameter,  $\phi$ , for Eq. 9.

The sediment graphs for the two selected cases, are given in Figs. 11 and 12. At the  $P = 3.8$  cm intensity (Fig. 12), the curves are essentially indistinguishable. This same pattern has been observed for hydrographs (not shown). However, as antecedent moisture and rainfall decrease, the differences are more prevalent (Fig. 11).

Estimates for  $\phi$  using the data in Figs. 11 and 12 are presented in Table

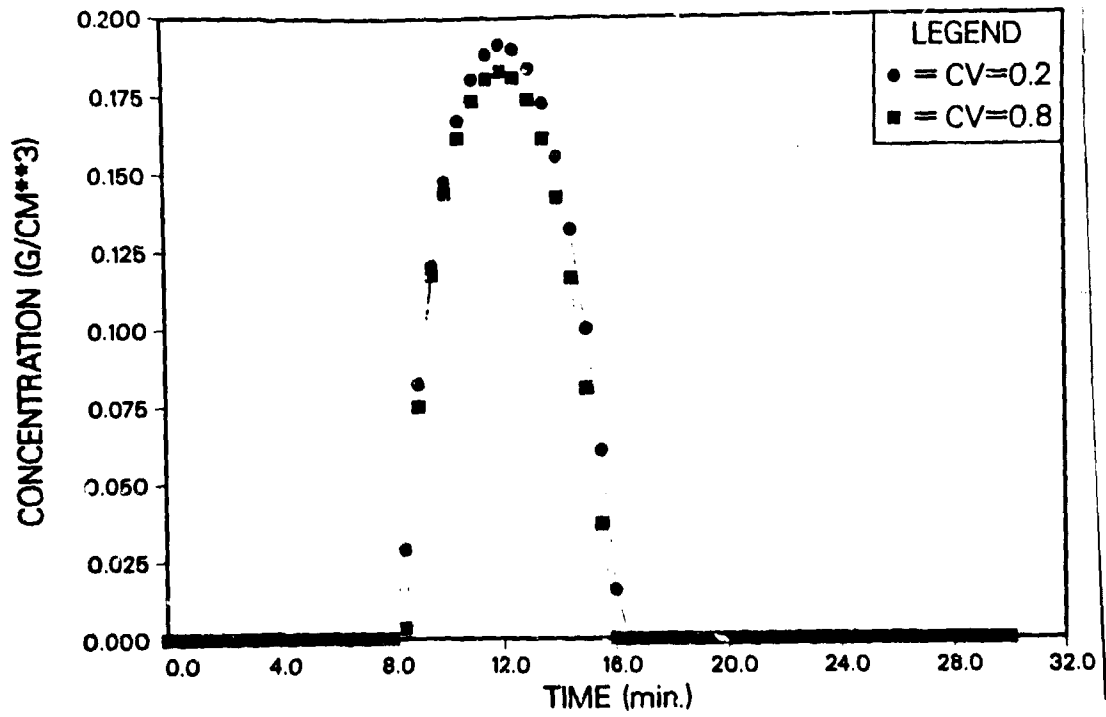


Figure 11.

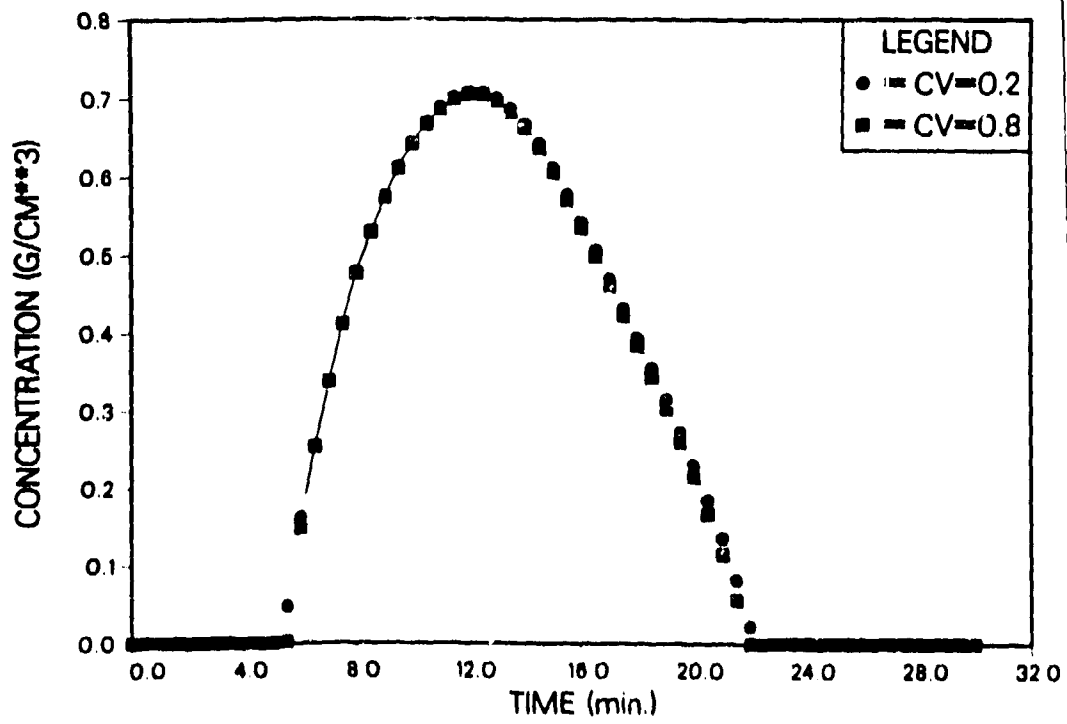


Figure 12.

3. The largest differences from the base value are seen for the case of  $P = 1.9$  cm.

Table 3. Optimized transport parameters for the DuBoys equation using a constant rather than distributed saturated hydraulic conductivity.

<u>Rainfall Intensity</u>	$\theta_1$	<u>0.2</u>	<u>CV</u> <u>0.8</u>
$3\bar{K}_s$	0.2	.0016	.0015
$6\bar{K}_s$	0.3	.0012	.0012

The estimates indicate that errors of 9 - 45% overestimation are introduced by neglecting the spatial distribution of  $K_s$  for these two cases. Computer simulation experiments have demonstrated that as antecedent moisture and/or rainfall intensity are increased, the differences in hydrographs from a hillslope described by a constant  $K_s$  and a hillslope with spatially variable  $K_s$  become indistinguishable. This same trend appears to occur for erosion. Another factor to be considered in the parameter estimation exercise is the assumption of perfect knowledge of the other parameters. In field situations these parameters will be measured or estimated from field data and these measurement errors will also be introduced into estimation process. As an example, if  $\bar{K}_s$  is underestimated by 10% for the case of  $CV = 0.8$ ,  $P = 1.9$  cm, and  $\theta_1 = 0.20$  produces an optimal estimate of  $\phi$  of 0.0011 which is the base case value from Table 1. A 10 percent overestimate of  $\bar{K}_s$  will give an optimal  $\phi$  value of 0.0026 for the same conditions. It should be expected that similar types errors may result in the estimation of the  $\alpha$  parameter in Eq. 6 and these will be carried into the estimation of  $\phi$ . So the results

presented here should be viewed as a best case in terms of erosion parameter estimation.

### Limitations

As with any simulation study, there are limitations in the interpretation of these results. The DuBoys equation was selected because it is simple in concept and application. More fundamental and physically-based detachment and transport models have been cited. Furthermore, only a small number of simulations have been presented. Thus, the effort in this study should be viewed as exploratory.

As shown in Figs. 2-10, considerable deposition and erosion were occurring along the hillslope, but no changes in slope bed or form were incorporated into the simulations. This leads to questions regarding the sheetflow assumption and the response of natural surfaces. In the simulations reported herein, the sheetflow assumption used in overland flow routing views the surface as a series, i.e., the upslope water is forced over downslope points. Experience from rainfall simulator experiments indicates that sheet flow may occur for only short before concentrating. Emmert (1970) traced flowlines on rainfall simulator plots showed this more graphically. The impact of concentrating the flow on erosion are potentially different than those seen in this study because the field system may respond in parallel. The need for a more complete simulator that can solve the two-dimensional St. venant Equations with spatially and temporally varying inflows is clear. Then changes in bed slope and form can be accommodated more readily into the simulations.

$K_g$  was the only variable spatially distributed in these simulations. Results from Springer and Cundy (1987) revealed that runoff hydrographs from simulations similar to these were not sensitive to the distributions of  $S_{av}$  or  $\theta_s$  so the mean value of these parameters could be used. One may view the ignoring of rainfall and runoff detachment processes and their associated spatial variability as a more critical limitation. Again, our belief is to start with the basic controlling processes and understand the impact of variability in them before moving on the next higher level. It is not possible, in our opinion, to discern the effects of spatial variability in rainfall or runoff detachment parameters until the effects for runoff generation or overland flow routing have been determined. Likewise, before sound principles can be derived for contaminant transport, the effects of spatially-varying soil erosion parameters will have to be understood.

## CONCLUSIONS

This preliminary study has provided some insight into erosion phenomenon on hillslopes with spatially variable infiltration. Among the conclusions are:

- 1) Spatial variability in  $K_g$  does lead to differential erosion and deposition along the slope.



- 2) Spatial variability in  $K_s$  leads to increased soil erosion when compared to the slope with uniform or constant  $K_s$ . This leads to bias in estimating erosion parameters using the uniform slope approximation.
- 3) As rainfall intensity or antecedent moisture increase differences in erosion between surfaces described by a spatially variable  $K_s$  and a uniform, average constant  $K_s$ , decrease. Increases in rainfall duration may play a similar role.
- 4) This study was very preliminary in nature. The limitations imposed by the overland flow routing assumptions have been discussed. The effects demonstrated in this study reinforce the need for a more complete overland flow routing scheme. A second point is the limited number of simulations that were conducted. A statistically designed Monte Carlo experiment is needed to better define the impacts of spatially variable  $K_s$ .

#### ACKNOWLEDGEMENT

This is a joint contribution of Los Alamos National Laboratory and the University of Washington. Support for the Los Alamos effort was provided by U. S. DOE, Office of Health and Environmental Research, Ecological Research Division, through the project, "Contaminant Transport in Southwestern Ecosystems". Los Alamos National Laboratory is operated by

the University of California for the U. S. DOE under contract  
W-7405-ENG-36.

#### REFERENCES

- Bennett, J.P. 1974. Concepts of mathematical modeling of sediment yield. *Water Resour. Res.*, 10:485-492.
- Brakensiek, D.L., and C.A. Onstad. 1977. Parameter estimation of the Green and Ampt infiltration equation. *Water Resour. Res.* 13:1009-1012.
- Cosby, B.J., G.M. Hornberger, R.B. Clapp, and T.R. Ginn. 1984. A statistical exploration of the relationships of soil moisture characteristics to the physical properties of soils. *Water Resour. Res.*, 20:682-690.
- Chu, S.-T. 1978. Infiltration during an unsteady rain. *Water Resour. Res.* 14: 461-467.
- Dagan, G., and E. Bresler. 1983. Unsaturated flow in spatially variable fields 1. Derivation of models of infiltration and redistribution. *Water Resour. Res.*, 19:413-420.
- Eggert, K.G. 1976. Modeling the unsteady infiltration process. M.S. Thesis. Colorado State Univ., Fort Collins, CO, 116p.

Foster, G.R., and L.D. Meyer. 1972. A closed-form soil erosion equation for upland areas. In Sedimentation: Symposium to Honor Professor H.A. Einstein. H.W. Shen, ed. Water Resour. Pub., Littleton, Co.

Foster, G.R., L.D. Meyer, and C.A. Onstad. 1977. An erosion equation derived from basic erosion principles. Trans. ASAE, 20:678-687.

Freeze, R.A. 1975. A stochastic-conceptual analysis of one-dimensional groundwater flow in nonuniform homogeneous media. Water Resour. Res., 11: 725-741.

Freeze, R.A. 1980. A stochastic-conceptual analysis of rainfall-runoff processes on a hillslope. Water Resour. Res., 16:391-408.

Green, W.H., and G.A. Ampt. 1911. Studies in soil physics. I. The flow of air and water through soils. J. Agric. Sci., 4:1-24.

Hawkins, R.H., and T.W. Cundy. 1987. Steady-state analysis of infiltration and overland flow for spatially-varied hillslopes. Water Resour. Bull. 23:251-256.

Henderson, F.M., and R.A. Wooding. 1964. Overland flow and groundwater flow from a steady rainfall of finite duration. J. Geophysical Res., 69:1531-1540.

Li, R.M., D.B. Simons, and M.A. Stevens. 1975. Nonlinear kinematic wave approximation for water routing. Water Resour. Res., 11:245-252.

Mein, R.G., and C.L. Larson. 1973. Modeling infiltration during a steady rain. *Water Resour. Res.*, 9:384-394.

Nielsen, D.R., J.W. Biggar, and K.T. Erh. 1973. Spatial variability of field-measured soil-water properties. *Hilgardia*, 42:215-259.

Rovey, E.W., D.A. Woolhiser, and R.E. Smith. 1977. A distributed kinematic model of upland watersheds. Colorado State Univ. Hydrology Paper No. 93, 52p.

SAS Institute. 1985. SAS user's guide: Basics. Version 5 edition. SAS Institute, Inc., Box 8000, Cary, NC. 1290p.

Simons, D.B., and F. Senturk. 1977. Sediment transport technology. *Water Resour. Pub.*, Littleton, CO.

Smith, R.E., and R.H.B. Hebbert. 1979. A Monte Carlo analysis of the hydrologic effects of spatial variability of infiltration. *Water Resour. Res.*, 15:419-429.

Smith, R.E., and J.-Y. Parlange. 1978. A parameter-efficient hydrologic infiltration model. *Water Resour. Res.*, 14:533-538.

Springer, E.P., and T.W. Cundy. 1987. Field-scale evaluation of infiltration parameters from soil texture for hydrologic analysis. *Water Resour. Res.*, 23:325-334.

Woolhiser, D.A., and D.C. Goodrich. 1988. Effects of storm intensity patterns on surface runoff. J. Hydrol. (in press)

## LIST OF FIGURES

- Figure 1. Conceptual view of the simulation surface.
- Figure 2. Cumulative erosion response for surface with coefficient of variation of  $K_g = 0.2$ , rainfall intensity =  $3\bar{K}_s$ , and initial water content = 0.2.
- Figure 3. Differential erosion response for surface with coefficient of variation of  $K_g = 0.2$ , rainfall intensity =  $3\bar{K}_s$ , and initial water content = 0.2.
- Figure 4. Cumulative erosion response for surface with coefficient of variation of  $K_g = 0.8$ , rainfall intensity =  $3\bar{K}_s$ , and initial water content = 0.2.
- Figure 5. Differential erosion response for surface with coefficient of variation of  $K_g = 0.8$ , rainfall intensity =  $3\bar{K}_s$ , and initial water content = 0.2.
- Figure 6. Cumulative erosion response for surface with constant  $K_g$ , rainfall intensity =  $3\bar{K}_s$ , and initial water content = 0.2.
- Figure 7. Differential erosion response for surface with constant  $K_g$ , rainfall intensity =  $3\bar{K}_s$ , and initial water content = 0.2.
- Figure 8. Cumulative erosion response for surface with constant  $K_g$ , rainfall intensity =  $6\bar{K}_s$ , and initial water content = 0.3.
- Figure 9. Differential erosion response for surface with coefficient of variation of  $K_g = 0.8$ , rainfall intensity =  $6\bar{K}_s$ , and initial water content = 0.2.
- Figure 10. Differential erosion response for surface with coefficient of variation of  $K_g = 0.2$ , rainfall intensity =  $6\bar{K}_s$ , and initial water content = 0.2.
- Figure 11. Sediment outflow graphs for surfaces with coefficients of variation of  $K_g = 0.2$  and 0.8, rainfall intensity =  $3\bar{K}_s$ , and initial water content = 0.2.
- Figure 12. Sediment outflow graphs for surfaces with coefficients of

variation of  $K_g = 0.2$  and  $0.8$ , rainfall intensity =  $6\bar{K}s$ , and  
initial water content =  $0.3$ .